Ab Initio Mechanical Properties of Alumina Polymorphs for Cold Spray Al Powder Passivation Layers

Cameron Crook[1*], Seyed Amirhossein Saeidi[1], Diran Apelian[1], Daniel Mumm[1], & Lorenzo Valdevit[1,2]

[1]Department of Materials Science and Engineering, University of California, Irvine, CA, USA
[2]Department of Mechanical and Aerospace Engineering, University of California, Irvine, CA, USA
*ccrook@uci.edu

Introduction

- Cold spray of aluminum powder is heavily influenced by particle passivation layers which must fracture for metallic bonding to occur.
- Previous work[1] identified powder particles treated under humid conditions had thicker passivation layers and the presence of hydration and partial crystallinity contributing to an increase in critical adhesion velocity (V_{cr}) of approximately 150 m/s.
- It is remains unclear whether crystallinity, thickness, composition or some combination are principally responsible.
- Experimental characterization of several nanometer thick passivation layers is prohibitively complex.
- Here, a first principles approach permits calculation of the mechanical properties for the majority of alumina polymorphs including oxide, hydrated, crystalline, and amorphous phases.

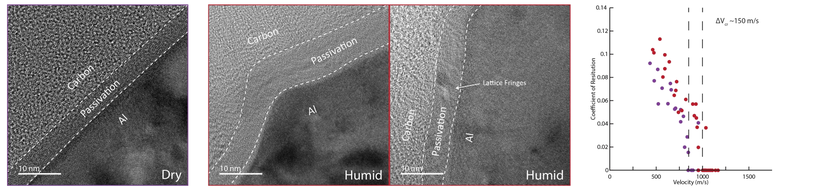

Computational Approach

- First principles static relaxation of polymorph structures is performed using Vienna Ab-Initio Simulation Package (VASP) [2] using the PBE functional[3].
- Crystalline phases, following initial relaxation, are homogeneously strained and relaxed under constant volume and cell shape to obtain their energy-volume relation.
- Bulk moduli are determined by fitting the Murnaghan equation of state[4]. For amorphous structures, this is done using the average of 20 simulations at 10 separate volumes.

$$E(V) = E_0 + K_0 V_0 \left[\frac{1}{K_0'(K_0'-1)} \left(\frac{V}{V_0}\right)^{1-K_0'} + \frac{1}{K_0' V_0} V - \frac{1}{K_0'-1} \right]$$

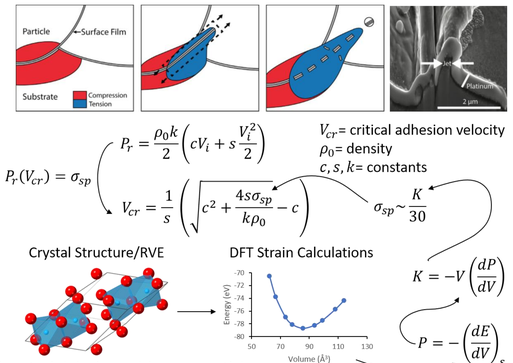

$$P_r(V_{cr}) = \sigma_{sp} \quad P_r = \frac{\rho_0 k}{2}\left(cV_i + s\frac{V_i^2}{2}\right) \quad V_{cr} = \frac{1}{s}\left(\sqrt{c^2 + \frac{4s\sigma_{sp}}{k\rho_0}} - c\right)$$

V_{cr}= critical adhesion velocity
ρ_0= density
c, s, k= constants

$$\sigma_{sp} \sim \frac{K}{30} \qquad K = -V\left(\frac{dP}{dV}\right) \qquad P = -\left(\frac{dE}{dV}\right)_s$$

Crystal Structure/RVE

DFT Strain Calculations

- Assuming high strain rates typical of the jetted material during cold spray particle impingement, the spall strength (σ_{sp}) is proportional to the bulk modulus (K) allowing estimation of the critical adhesion velocity using shock [5].
- Amorphous microstructures are generated using molecular dynamics via a melting (6000° K, sampling every 100 fs after equilibrium is reached) and quenching (6000 - 300° K, -1.5 K/fs) scheme with a ReaxFF potential[6] incorporating aluminum ions in LAMMPS[7] followed by static relaxations using VASP.
- The radial distribution function, $g(r)$, is used to confirm the simulations produce amorphous microstructures.

$$g(r) = \frac{1}{N_\alpha N_\beta} \sum_i^{N_\alpha} \sum_j^{N_\beta} \langle \delta(r_i - r_j) \rangle$$

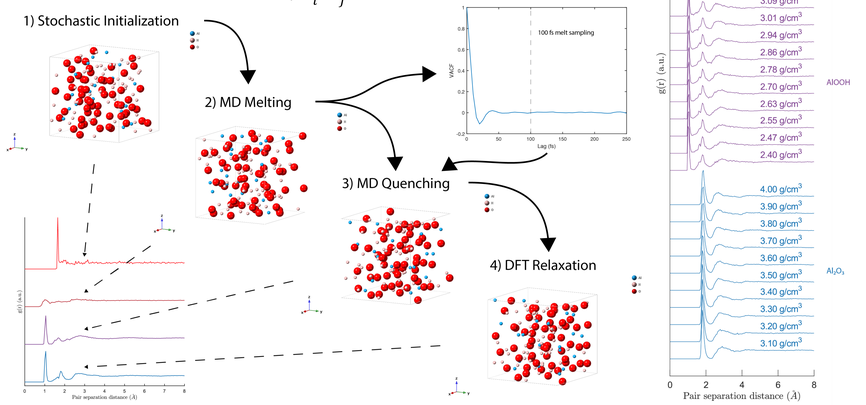

Results

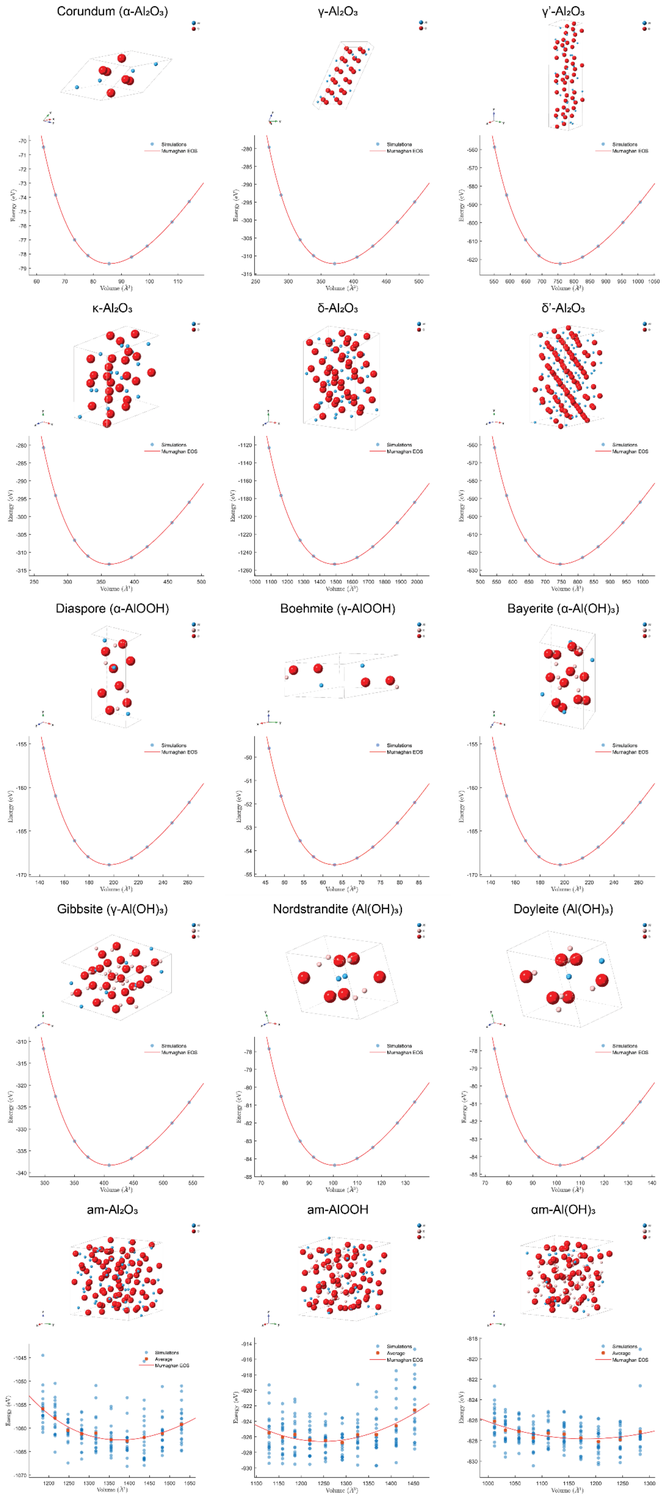

- Bulk modulus is highest, as expected, for thermodynamically stable α-Al_2O_3 and lowest for am-$Al(OH)_3$.
- The bulk moduli do not differ significantly within crystalline transition oxides or crystalline oxyhydroxides and hydroxides.
- The largest variations in bulk moduli are observed across crystalline and amorphous phases.
- Assuming the jetted material at the boundary of the particle-substrate interface is purely in tension and the observation that the jet is nominally 100 nm across, a simple rule-of-mixtures is used to approximate the spall strength of the interface and thus the critical adhesion velocity using the following values: $\sigma_{Al} = 1.02$ GPa[9], $V_{cr,dry} = 850$ m/s[1], $f_{pass,humid} = 0.08$[1], and $f_{pass,humid} = 0.05$[1].

$$V_{cr} \propto \sigma_{sp,jet} \propto \sigma_{Al}\left(1 - f_{pass}\right) + \frac{K_{pass}}{30} f_{pass} = \sigma_{Al}\left(1 - f_{pass}\right) + \sigma_{pass} f_{pass}$$

$$\Delta V_{cr} = V_{cr,dry}\left[\frac{\sigma_{Al}\left(1 - f_{pass,humid}\right) + \frac{K_{pass}}{30} f_{pass,humid}}{\sigma_{Al}\left(1 - f_{am-Al_2O_3}\right) + \frac{K_{am-Al_2O_3}}{30} f_{am-Al_2O_3}} - 1\right]$$

- Amorphous AlOOH and $Al(OH)_3$ result in a reduction in critical adhesion velocity despite a thicker passivation layer.
- Note that the formula above is very sensitive to thickness (i.e. f). In this approximation, passivation layers are treated as uniform and smooth. However, thickness variations were previously observed in micrographs of the humidity treated passivation layer.
- A fully crystalline passivation layer regardless of composition would have a significantly higher critical adhesion velocity.

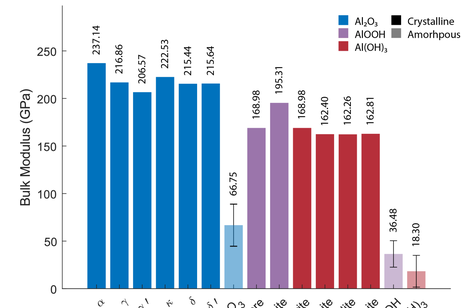

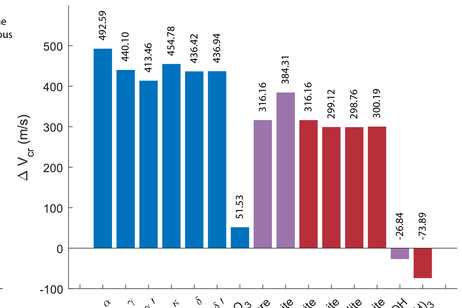

Conclusions

- Given the lower bulk moduli of both amorphous and crystalline (oxy)hydroxides compared to the oxides, the critical adhesion velocity is expected to decrease and therefore does not explain the results of experiments.
- Rather, it seems hydration plays an integral role in the accelerated passivation layer growth at low temperatures.
- Likewise, the bulk moduli of crystalline oxides do not significantly differ. Though am-Al_2O_3 is thermodynamically stable below ~10 nm, above that γ-Al_2O_3 becomes more favorable[8], meaning any crystallinity significantly increases V_{cr}.
- As previous micrographs show, the presence of partial crystallinity in passivation layers ~8-10 nm thick points to thickness and crystallinity being the principle drivers of increases in critical adhesion velocity.

Acknowledgements

This work utilized the infrastructure for high-performance and high-throughput computing, research data storage and analysis, and scientific software tool integration built, operated, and updated by the Research Cyberinfrastructure Center (RCIC) at the University of California, Irvine (UCI). The RCIC provides cluster-based systems, application software, and scalable storage to directly support the UCI research community. Funding was provided by ARL under contract grant number W911NF-19-2-0108.

References

[1]Lienhard et al. (2020) Acta Mater. 197
[2]Kresse et al. (1996) Phys. Rev. B 54
[3]Perdew et al. (1996) Phys. Rev. Lett. 78
[4]Murnaghan (1937) Am. J. Math. 59
[5]Hassani-Gangaraj et al. (2018) Acta Mater. 158
[6]Sen et al. (2013) Appl. Phys. Lett. 102
[7]Aktugla et al. (2012) Pa rallel Comput. 38
[8]Aykol et al. (2018) ACS Appl. Mater. Interfaces 10
[9]Eliezer et al. (1997) AIP Conf. Proc. 406